



Harmonized mapping of forests with a protection function against rockfalls over European Alpine countries

S. Dupire, D. Toe, J.-B Barré, F. Bourrier, F. Berger

► To cite this version:

S. Dupire, D. Toe, J.-B Barré, F. Bourrier, F. Berger. Harmonized mapping of forests with a protection function against rockfalls over European Alpine countries. 2020. hal-02519495

HAL Id: hal-02519495

<https://hal.archives-ouvertes.fr/hal-02519495>

Preprint submitted on 26 Mar 2020

HAL is a multi-disciplinary open access archive for the deposit and dissemination of scientific research documents, whether they are published or not. The documents may come from teaching and research institutions in France or abroad, or from public or private research centers.

L'archive ouverte pluridisciplinaire **HAL**, est destinée au dépôt et à la diffusion de documents scientifiques de niveau recherche, publiés ou non, émanant des établissements d'enseignement et de recherche français ou étrangers, des laboratoires publics ou privés.

Harmonized mapping of forests with a protection function against rockfalls over European Alpine countries

S. Dupire^{a,*}, D. Toe^a, J.-B. Barré^a, F. Bourrier^b, F. Berger^a

^aUniv. Grenoble Alpes, INRAE, LESSEM, 38000 Grenoble, France

^bUniv. Grenoble Alpes, INRAE, ETNA, 38000 Grenoble, France

Abstract

Forest covers 40% of the European Alpine region and contributes to the protection of human beings and infrastructures against natural hazards such as rockfalls. However, despite the recognition of this ecosystem service, most mountain territories do not have a map of protection forests. When a map exists, it generally depends on data restricted to a limited extent, which prevents any replication or comparison on other areas.

The aim of this study is to develop a method using harmonized and open data to produce the first map of protection forests against rockfalls at the European Alpine region scale. Based on these data, we first identified potential rockfall release areas and calibrated the model according to 2812 real rockfall events located around the Alps. Second, 46.5 billion 3-D rockfall propagation simulations, taking into account topography, land use and human assets, were computed on the entire area. Protection forest is defined as being located on at least one rockfall trajectory that had impacted human assets.

Our results show that 14% of the forests have a potential protection function against rockfalls in the Alpine Space region. This proportion goes up to 21.5%, if we consider only the core of the Alpine area. 80% of the protection forest area contributes to mitigate rockfall hazard on road network, 55% on buildings and only 6% on railways. This work provides a robust, objective and reproducible method for locating protection forests on a large geographical scale. Such a map may serve as a basis for national and European risk management policies.

Keywords: Protection forests, Rockfall, Mapping, Ecosystem services, Alps, Natural hazard

Highlights

- We identified harmonized open data to model rockfall propagation over European Alps
- 46.5 billions rockfall trajectories were computed to identify protection forests
- 14% of protection forests in the Alpine region (21.5% in the core of the Alpine area)
- 80% of protection forests area protect roads, 55% buildings and 6% railways
- Reproducible method and result available for policy makers, foresters and risk managers

*Corresponding author at: INRAE, UR LESSEM, 2 rue de la Papeterie-BP 76, F-38402 St-Martin-d'Hères, France
Email address: sylvain.dupire@inrae.fr (S. Dupire)

1. Introduction

Mountain forests provide many ecosystem services (Briner et al., 2013), including the protection of human beings and infrastructures against natural hazards. In the Alpine region, the role of forests is often considered equivalent to civil engineering measures as it represents a cost-effective solution (Notaro and Paletto, 2012) especially to mitigate avalanches, soil erosion or rockfalls (Bebi et al., 2001; Brang et al., 2001).

The preservation and enhancement of the role of forests in mitigating natural hazards is essential in the strategies for the protection of inhabitants, users and economic activities of the mountain territories (Accastello et al., 2019). The ongoing climate changes may promote disturbances such as fires (Dupire et al., 2019, 2017; Conedera et al., 2018), wind-storm (Csilléry et al., 2017) and drought (Gobron et al., 2005). In order to avoid their catastrophic consequences related to the alteration, or even the disappearance, of the forest cover (Gehring et al., 2019), it is first of all necessary to locate the forests that have a protective role, which requires a cartographic zoning of this ecosystem service (Lepuschitz, 2015).

Different regional-scale maps of rockfall hazard have been proposed (Toe and Berger, 2015; Acosta et al., 2007), but they are not adapted to identify the forests with a potential effect on rockfall hazard mitigation. On the other hand, Switzerland (Losey and Wehrli, 2013) and more locally certain administrative regions in the Alpine region (Getzner et al., 2017; Meloni et al., 2006) have maps of protection forests but the natural hazard(s) against which forests protect are not always well informed. In addition, these maps are developed using different methods and input data from different sources making it nearly impossible to compare the results from one area to another. Thus, despite the recognition of the protection effect of forest against rockfall in both national and European forest policies, there is currently no harmonized method for carrying out such mapping.

In this context, our study shares the objective of the Alpine Space project "RockTheAlps"¹ which aims to produce the first harmonized map of protection forests against rockfalls at the European Alpine Region scale. For this purpose, we first identified opensource and harmonized spatial data available for the entire study area. Second, 3-D rockfall simulations were conducted on 6 pilot areas in order to calibrate the rockfall model parameters. Third, rockfall simulations were computed on the whole study area and allowed to identify and locate the protection forests. Finally, we analysed the proportion of protection forests and human assets at risk at different scales.

2. Material and methods

2.1. Study area

This study focuses on the European Alps which geographical extent may be defined according to geographical, economical and cultural criteria (Fig. 1). Two areas of analysis were used in this work. The first one corresponds to the Alpine Region as defined by the European Alpine Space programme (www.alpine-space.eu). This area is based on administrative borders and is characterized by 188 Units for Territorial Statistics (referred as NUTS3) covering 390 227 km² over 8 countries (Austria, France, Germany, Italy, Liechtenstein, Monaco, Slovenia and Switzerland). NUTS3 refers to the hierarchical system used to divide up the economic territory of the European Union for the collection, development, and harmonization of socio-economic analyses of small regions (< 800 000 inhabitants).

The second area of analysis is defined by the Alpine Convention (www.alpconv.org) whose extent better fits to the orographic contours of the Alps. This area covers 190 717 km² and excludes the flattest regions present in the Alpine Space programme (e.g. Po Plain and Rhone Valleys).

2.2. General model description

This section describes the general workflow (Fig. 2) used to establish the harmonized mapping of protection forests against rockfalls and specifies the inputs and outputs of the model. Details on the process itself are given in section 2.3.

¹ www.alpine-space.eu/projects/rockthealps/en/home

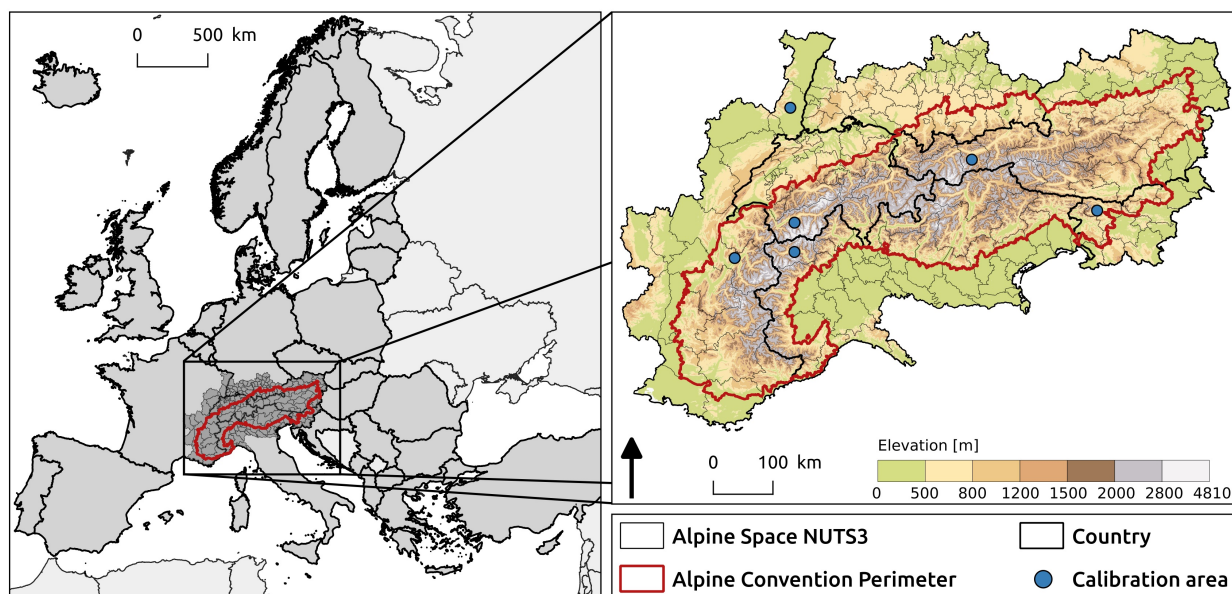


Figure 1: Map of the Alpine Space area and Alpine convention perimeter (red line).

2.2.1. Input sources

Spatial input data were chosen to be harmonized over the entire study area and in open access. Therefore, they were taken from two main sources: the European Union’s Earth Observation Programme Copernicus² and OpenStreetMap³.

Relief and topography were obtained from the EU-DEM⁴ v1.1 which is a digital terrain model (DTM) available in raster format for Europe at 25m spatial resolution with an overall vertical accuracy of 2.9 meters RMSE. EU-DEM was used as is to account for relief and topography in the modelling process. A slope raster was also produced from this source in order to identify the potential rock release areas (see section 2.3.1).

Land and forest cover were extracted from Corine Land Cover (CLC) 2018⁵ (Büttner and Kosztra, 2017). CLC is produced by visual interpretation of high resolution satellite imagery. It is available in shapefile (vector layer of polygons) format with a minimum mapping unit of 25 ha. The forest area input was derived from CLC by extracting entities with the CLC level 3 codes in [311, 312, 313, 323, 324]. CLC was also used to develop the classification of soil types (see section 2.3.3).

Water surfaces and rivers were obtained from © OpenStreetMap contributors in shapefile format and used also to develop the classification of soil types.

Human assets were taken from © OpenStreetMap contributors locating different topographical information over the world. The assets used were of three types (see Table 1) and were saved in four layers in shapefile format. No detailed information was available in OpenStreetMap in order to distinguish the different types of buildings (e.g. houses, schools, industry, etc.). Thus, we assumed the same vulnerability to rockfall for all buildings. Moreover, there was no information about linear assets that are already protected from rockfall with permanent civil engineering fences such as embankments. Therefore, linear assets were assumed to be vulnerable to rockfall on their entire length. Human asset shapefiles were rasterized at the EU-DEM resolution for the modelling process and were also used for the elaboration of soil classes. The rasterization process allowed to keep a trace of the type of asset present on each

²<https://land.copernicus.eu/>

³<https://www.openstreetmap.org/copyright/en>

⁴<https://land.copernicus.eu/imagery-in-situ/eu-dem>

⁵<https://land.copernicus.eu/pan-european/corine-land-cover>

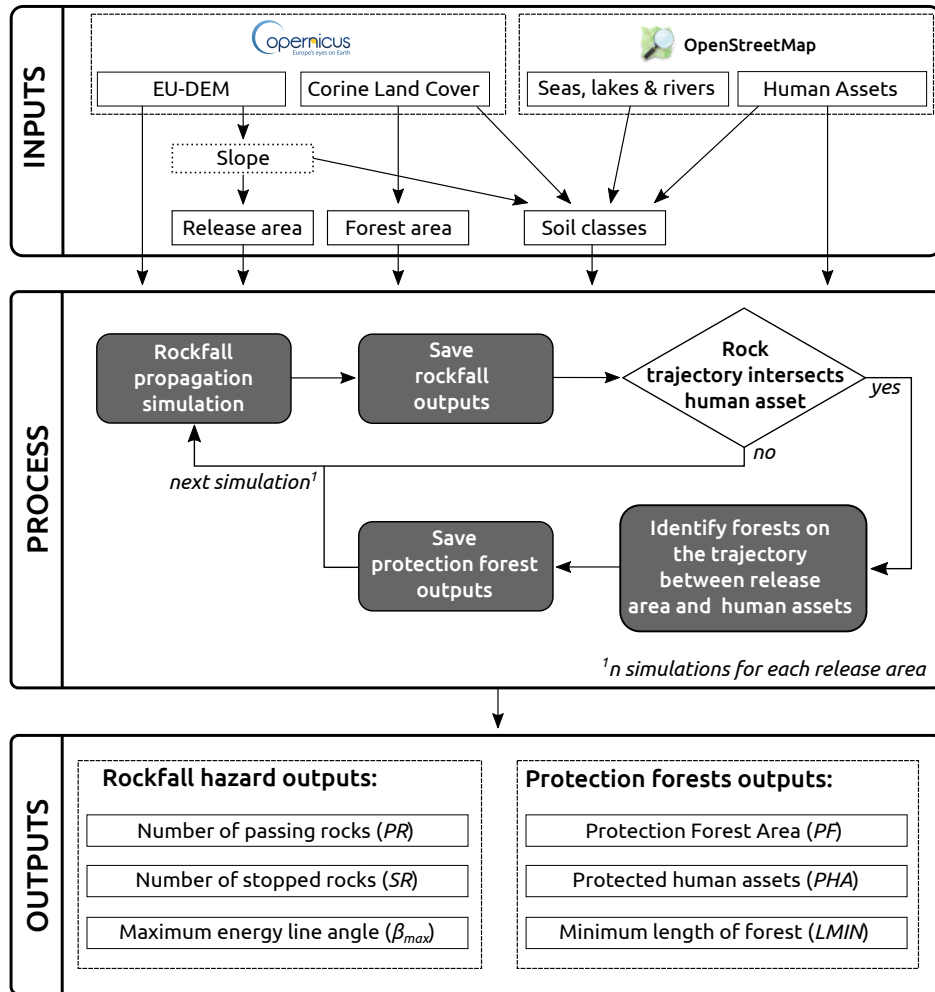


Figure 2: General workflow used for the harmonized mapping of protection forests.

Table 1: Description of the human assets used for mapping protection forests.

Human asset type	Description	Shape	Code
Railways	National or regional railway lines	Line	1
Buildings	Houses, socio-economic complexes, infrastructures	Polygon	10
Main roads	Highways + national or regional roads	Line	100

raster cell. For example, if buildings and road are present on the same raster cell, it will have the code 110 (10 for Buildings + 100 for Roads).

2.2.2. Process

The propagation on the slope of 500 rocks with a random volume between $[0.1, 5] \text{ m}^3$ is modeled from each pixel identified as release area (see section 2.3.1). This range of volume corresponds to the optimal efficiency of forests against rockfalls (Berger et al., 2002). The propagation of rocks down the slope is simulated on the rasterized digital terrain model (EU-DEM) by successive sequences of free flights through the air and rebounds on the slope surface (see section 2.3 for detailed description). For each rockfall simulation, the rock volume was randomly taken in the previous range and outputs relative to rockfall activity are systematically saved on the rock trajectory. If the rock

trajectory intersects a human asset, all the pixels of forest located between the asset and the release area are mapped as protection forest.

2.2.3. Outputs

The simulation outputs are made up of two sets of results. The first set gathers **Rockfall hazard outputs** which consist in three 25 m resolution rasters. It is only used to calibrate (see section 2.4) and validate (see section 2.5) the modelling process. The first raster returns the number of passing rocks for each raster cell located on a simulated rock trajectory. The second refers to the raster cells where rocks ended their courses. Finally, the last raster gives the maximum energy line angle (see section 2.4 for definition) observed for each cell with a passing rock. It is important to underline that these data are adapted to identify forests with a protective function but not intended to be used for hazard zoning or risk assessment.

The second set concerns **Protection forest outputs** which are the final expected results of this study. They consists in three datasets. The first one is a shapefile locating the protection forests. The second is a raster at 25 m resolution returning the human assets type protected by the forest. Finally, a 25 m resolution raster inform on the minimum length of forest present between the release areas and the human assets for each pixel of protection forest.

2.3. Detailed model description

2.3.1. Rockfall source area identification

A classical approach to determine the potential rockfall sources consists in identifying the areas with a slope angle greater than a given threshold value (Frattini et al., 2008; Dorren and Seijmonsbergen, 2003). The value of this threshold angle highly depends on the geomorphology as well as the quality and resolution of the slope raster (Michoud et al., 2012). For example, a vertical cliff of 10 m will be represented by slope values between 82° and 84° on a 1 m grid cell (depending on the cliff aspect) and slopes values between 16° and 22° on a 25 m grid cell (Loye et al., 2009). Therefore, standard DEM (25 m resolution), such as the EU-DEM, considerably smooths the relief which makes difficult the identification of precise rockfall source areas. To overcome this issue, six calibrations areas spread over the Alpine Space (Table. 2) were used to identify the slope angle threshold to be used at the Alpine Space level. 1 m DEM derived from Lidar was available for each area and used to identify potential rockfall source pixels using a threshold slope angle of 50°. This value corresponds to the average obtained on the different geomorphological areas analysed at 1 m resolution by Loye et al. (2009). These potential source areas were rasterized at the same resolution as slope raster derived from EU-DEM (25 m) in order to extract the slope angle distribution on their location. The distributions obtained considerably vary between the calibration zones (Table. 2) which conducted us to choose two thresholds to be applied at the Alpine Space scale that correspond to the 25th and the 75th percentiles of the distribution considering all the calibration zones.

Table 2: 25 m DEM-based slope Angle obtained on potential rockfall sources identified from Lidar data on the different calibration areas. Locations of the different areas are displayed in Fig. 1.

Zone	Area [km ²]	EU-DEM Slope angle (25m) [°]	
		25th percentile	75th percentile
AT - Innsbruck	2096	30	43
CH - Valais	6117	29	42
IT - Valle d' Aosta	3262	29	43
FR - Savoie (Bauges)	1614	27	40
FR - Bas-Rhin (Vosges)	1364	19	31
SI - Gorenjska	2168	23	39
All zones	16621	28	42

The first threshold of 42° is more likely to identify release areas in mountainous terrain and is in agreement with the values found in the literature for mountain areas which stand in the range [40–45°] at a 25 m resolution (Dumperth et al., 2016; Loye et al., 2009; Acosta et al., 2007; Dorren and Seijmonsbergen, 2003). The second threshold of 28° is mostly interesting in mid-mountains and pre-Alps where the EU-DEM relief may be too smoothed to identify source areas as shown by the slope angle distribution of the FR-Bas-Rhin (Vosges) calibration area.

Ultimately, 9756 km² (15.6 million pixels) for release areas on slopes greater than or equal to 42° and 48388 km² (77.4 million pixels) for release areas on slope in the range [28-42°] were detected on the entire Alpine Space region. As 500 rockfall simulations are launched by release area, it resulted in 46.5 billion rockfall trajectory simulations.

2.3.2. Model of rock propagation and rebounds on the slope surface

The block propagation is modeled by a succession of free flights and impacts on the slope surface. During the free flight phase, as the block is only subjected to gravity, its trajectory can be described as a parabola depending on the velocities at the beginning of the flight phase and on the acceleration due to gravity (g) (Bourrier et al., 2012).

The computation of the rebound on the soil is made of two steps. The first step enables to calculate the block deviation after impact according to its incoming trajectory and the slope (Dorren et al., 2006). The second step enables to calculate the translational and rotational velocities of the block after an impact on the soil depending on the incident block velocities and soil classes. It is based on the rebound model developed by Pfeiffer and Bowen (1989). The normal and the tangential components of the velocity after impact are calculated as functions of the normal, tangential and rotational components of the velocity before impact, two restitution coefficients (R_n and R_t), and the block characteristics (mass, diameter and inertia). R_n values are directly associated with the 7 soil classes proposed. R_t is calculated using the roughness of the soil (R_g), the block radius, and the penetration depth of the block in the soil (Dorren et al., 2006, 2004). Consequently, the block propagation is depending on two parameters related to soil properties: the normal restitution coefficient R_n and the soil roughness R_g .

2.3.3. Definition of soil classes

Soil parameter values used in rockfall propagation model are often derived from the type of land use (Dorren, 2015; Volkwein et al., 2011). Corine Land Cover provides a homogeneous description of land use at the European scale and it is therefore the main input of the soil classes proposed in this study (Fig. 3). 8 soil classes (SC) were defined from CLC and precised according to elevation, slope or vector information on human assets, water surfaces and rivers. The SC (I) corresponds to agricultural area characterized by deep soils with a high capacity to reduce rockfall velocity. SC (II) are associated to forest area defined by a high diversity of soil structures in terms of depth, damping capacity and surface roughness. SC (III) represents mineral area, glacier and high elevation meadows. It is characterized by a wide range of soil parameters promoting rock propagation. SC (IV) gathers CLC codes linked to human activities and urban areas. SC (V) concerns permanent water area and rivers where rock propagation is stopped ($R_n=0$). SC (VI) corresponds to temporary water area such as bog or mountain torrent with intermittent regime and are characterized by a low rock propagation. SC (VII) are associated to screes - i.e. CLC codes corresponding to mineral surface but located on slopes in the range $[32,40]^\circ$ (Francou and Manté, 1990) - and are defined by a high surface roughness. Finally SC (VIII) represents meadows, shrub-lands and grasslands from low to middle elevation (< 2000 m) characterized with soil depths and rock propagation in between those of forests and mineral areas.

2.3.4. Identification of potential protection forests

At the beginning of the simulation process, three rasters of the same size and resolution as the DEM are created. The first (*PF*) is initialized to zero and will be used to identify the protection forest pixels (which will be coded 1). The second raster (*LMIN*) will store the minimum length of forest on the slope between the source area and the human assets. The last one (*PHA*) is initialized to zero and will identify the types of human assets protected by the forest.

During the propagation simulation, the trajectory of each block (*traj*) is temporarily recorded as it progresses. Each time a raster cell is added to the trajectory, a test is performed to determine if human assets are located at that position. If yes, all forest pixels located on the path upstream of the human asset (*trajFor*) are identified as protective forest: $PF[trajFor]=1$. The length of forest between the starting area and the stake (L) is also calculated. The minimum values between L and those contained in *LMIN* for each forest cell on the trajectory are kept: $LMIN[trajFor] = \min(LMIN[trajFor], L)$. Finally, the code of the human asset type (see Table. 1) is added to each *PHA* forest raster cells on the trajectory: $PHA[trajFor]=PHA[trajFor]+code$. With this process, if a forest protects both a building (code 10) and a road (code 100), *PHA* will get the code 110.

2.4. Calibration of soil parameters for rockfall propagation

The calibration of rockfall propagation model consisted in defining the range of normal restitution coefficient R_n and soil roughness R_g for each soil class based on the distribution of the energy line angle. The energy line principle has been first described by Heim (1932) before being used in several rockfall applications (Toe and Berger, 2015; Berger and Dorren, 2007). The energy line is characterized by the angle β between the horizontal plane and a fictive line drawn between the top of a rockfall source to the stopping point β is easy to measure on the field and can provide

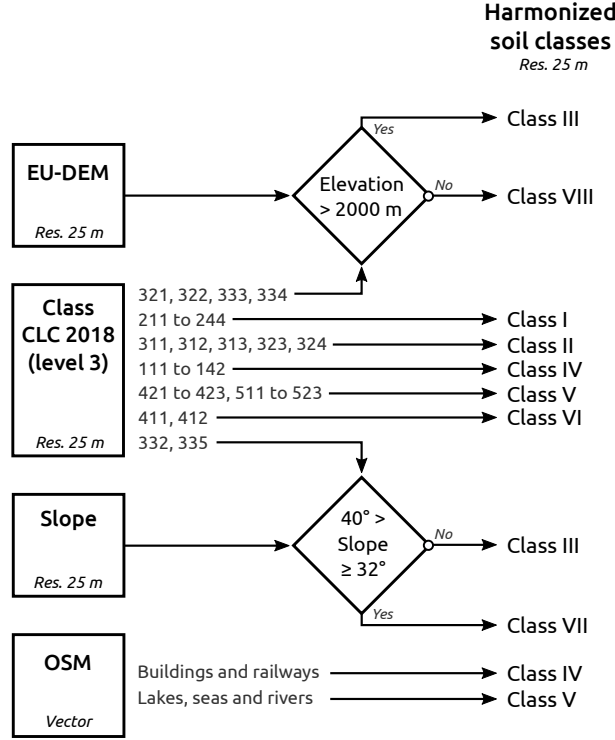


Figure 3: Chart of assignment of soil classes.

a rough statistical estimation of the rockfall run-out distance. In the framework of the Interreg - Alpine Space project *RockTheAlps*, a collection of rockfalls events across the Alps is carried out. This database (still in progress) gathers information on rockfalls events such as date of the event, rock volume, energy line angle β , location of source, location of stop and complete ground profile (not all the information is systematically known for each event). At the time of the study, β was available for 2812 rockfall events.

The model returns as output a raster of maximum energy line angle (β_{max}) which identifies for each cell on a block trajectory the maximum of all energy line angles β observed. Another output is a raster of stopped rocks (SR) returning the number of rocks that stopped their courses in each cell. Therefore, for each simulation, it is possible to obtain a distribution of the β angle by extracting the values of β_{max} on the cells with $SR > 0$.

The objective of the calibration step was to obtain a high level of similarity between observed distribution (β values observed on 2812 real rockfall events) and the modeled distribution calculated from β_{max} and SR obtained with the simulations of rock propagation from release areas on slopes $\geq 42^\circ$ (the most suitable to Alpine region, see section 2.3.1) on the 6 areas defined in Table.2. The similarity was assessed with two different criteria. First, we used a Wilcoxon rank sum test (Hollander et al., 2013; Wilcoxon, 1945) in order to center the modeled distribution on the observed values. Second, the Bhattacharyya coefficient (BC) (Bhattacharyya, 1946) was applied to calculate the probability of distribution overlap. Its expression is given by:

$$BC(p, q) = \int \sqrt{p(x) \cdot q(x)} dx \quad (1)$$

where $p(x)$ and $q(x)$ are the probability density functions to be compared. BC takes values between 0 (distributions do not overlap) and 1 (complete similarity).

In practice, different rockfall propagation simulations were carried out on the 6 calibration areas where soil parameters R_n and R_g were adjusted in order to have a conclusive Wilcoxon test (p-value $\ggg 0.05$) and a $BC > 0.95$ for simulations from release areas located on slopes $\geq 42^\circ$.

2.5. Validation of soil parameters for rockfall propagation

The modeled distributions of the energy line angle β on the entire Alpine Space area were analysed and compared to the same observed distribution used for model calibration. Modeled distributions were split according to the release area source and their similarity with the observed values was assessed using Wilcoxon rank sum test and Bhattacharyya coefficient as described previously in section 2.4.

In addition to the previous point, we intersected the modeled propagation area (output raster of the number of passing rocks PR) with the locations of the deposits of real rockfalls events from the RockTheAlps database. 3685 events located in France, Italy and Slovenia were available at the time of this study. The distance between each real rockfall events to the nearest modeled propagation area was also computed in order to analyse the different plausible causes of non-intersection.

3. Results

3.1. Calibration and validation of the rockfall propagation model

3.1.1. Analyse of energy line angle distributions

Fig. 4 and Table. 3 return the results of the calibration and the validation steps regarding the distribution of the energy line angle β .

Table 3: Results of the statistical tests used to compare the energy line angle distributions. Observed distribution concerned the β angle of the 2812 rockfall events in the RockTheAlps database. The calibration set corresponds to the β angle distribution modeled on the 6 calibration areas (see Table.2). The validation set concerns the β angle distribution modeled on the entire Alpine Space area. Difference is made between rockfall simulations from release areas located on slopes $\geq 42^\circ$ (suitable to the Alpine region) and those on slopes in the range $[28-42[$.

	Release areas: slopes $\geq 42^\circ$		Release areas: slopes in $[28-42[$	
	Calibration set	Validation set	Calibration set	Validation set
Wilcoxon p-value*	0.48	0.99	$<10^{-16}$	$<10^{-16}$
Bhattacharyya coefficient	0.98	0.96	0.85	0.81

*Null hypothesis: True location shift is not equal to zero

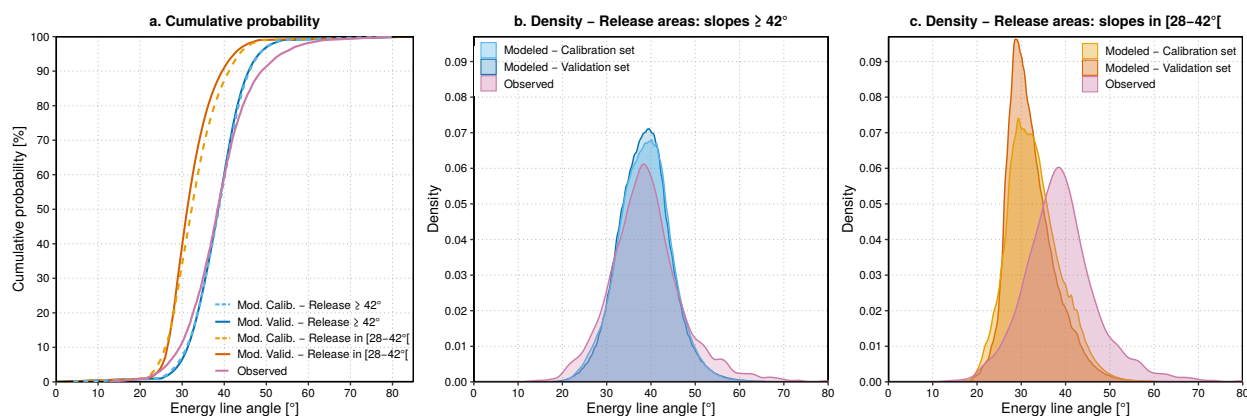


Figure 4: Distributions of the energy line angle β of observed rockfall events and modeled rockfall propagations. Modeled distributions are split according to the slope of the release areas and between calibration (6 areas described in Table.2 in dotted lines) and validation sets (entire Alpine Space region in full line). Cumulative probability curves (a.) and comparisons of density curves between observed and modeled β distributions for release areas in slopes $\geq 42^\circ$ (b.) and slopes in $[28-42[$ (c.) are displayed.

According to the statistical tests, observed and modeled distributions for release areas in slopes $\geq 42^\circ$ have similar distributions. Non-significant difference are observed in median values (0.2° for calibration set – 0.1° for validation set) as well as a high probability of distribution overlap (for both calibration and validation $BC > 0.95$). The standard deviation is however greater in the observed (8.15°) than in the modeled distributions (5.97° for calibration set – 5.88° for validation set).

for validation set). These results suggests that the soil parameters used to model the propagation of the rocks are suitable for the Alpine region.

In contrast to the modeled distributions for release areas in slopes $\geq 42^\circ$, those for release areas in slopes in the range $[28-42^\circ]$ presented lower values of β angle than to the observed distribution (difference in median of -6.16° for calibration set and -7.21° for validation set). The modeled β angle values are also less scattered than observed values.

3.1.2. Final parameters of the soil classes

The ranges of R_n and R_g obtained after calibration process and used for the mapping of protection forests on the whole study area is shown in Table 4.

Table 4: Optimal values of R_n and R_g for each soil class obtained during the calibration process.

Soil class	Description	R_n range[-]	R_g range [m]
I	Agricultural area	0.23 – 0.31	0.05 – 0.18
II	Forest area	0.30 – 0.42	0.05 – 0.23
III	Mineral area	0.39 – 0.58	0.05 – 0.13
IV	Urban area	0.32 – 0.39	0.10 – 0.58
V	Permanent water area	0	0
VI	Temporary water area	0.30 – 0.42	0.40 – 0.48
VII	Screes	0.39 – 0.58	0.15 – 0.33
VIII	Meadows and grassland	0.30 – 0.42	0.05 – 0.18

3.1.3. Analysis of the run-out distance: comparison with real rockfall events

90% of the 3685 real rockfall events were located inside the modeled rockfall propagation area (Fig. 5). 65% of the real events intersected the propagation areas from release areas in slopes $\geq 42^\circ$ and 25% in the propagation areas from release areas in slopes in $[28-42^\circ]$.

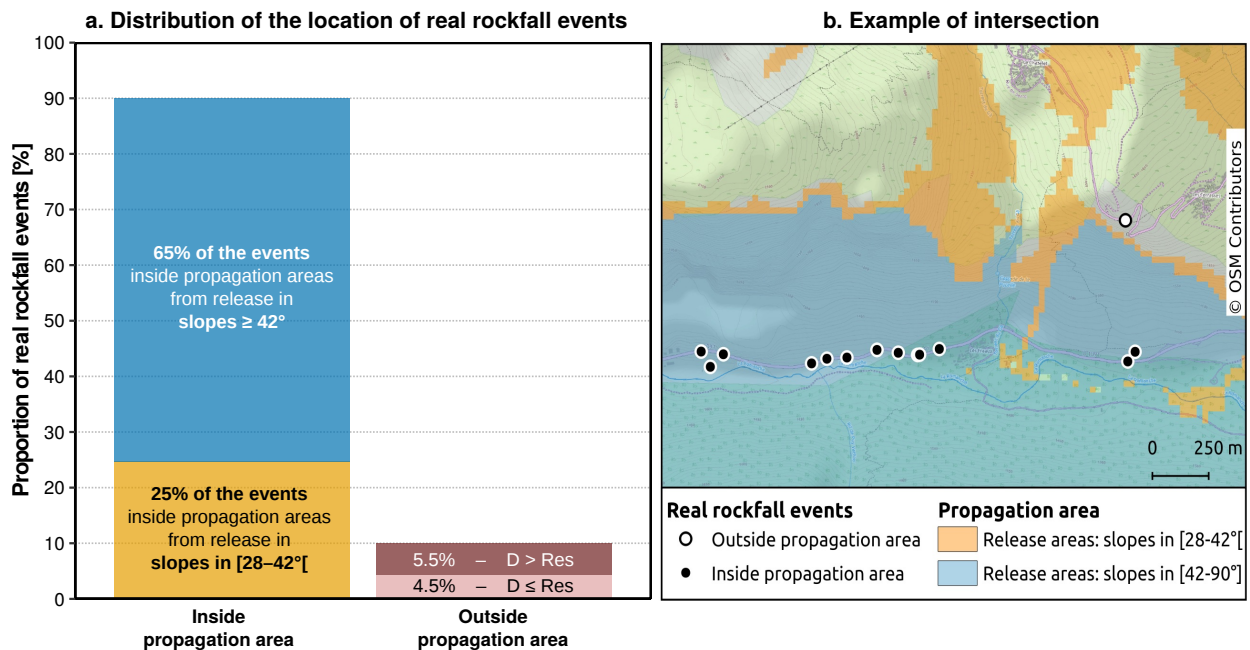


Figure 5: Results of the spatial intersection between modeled propagation areas and location of real rockfall events (a.). Difference is made between propagation areas according to the slope threshold taken into account to identify the release zones. When outside the propagation area, difference is made between the events within a distance to the nearest modeled propagation area (D) less than or equal to the size of the working raster resolution (Res equal to 25 m) and those located beyond. An example of intersection in Isère (France) is also given (b.).

Only 10% of the real rockfall events did not intersect modeled rockfall propagation areas. Nonetheless, about half of them were located close to a propagation area, e.g. within a distance less or equal than the raster resolution of 25 m.

3.2. Results of the harmonized mapping of protection forest against rockfalls

All mapping results as well as thematic maps are freely available for downloading on the RockTheAlps project [website](#).

When all release areas are considered, 92% of the protection forests of the Alpine Space region are located into the restricted perimeters of the Alpine Convention. This proportion is higher with 97% of the protection forests when only release areas on slopes greater than or equal to 42° are considered.

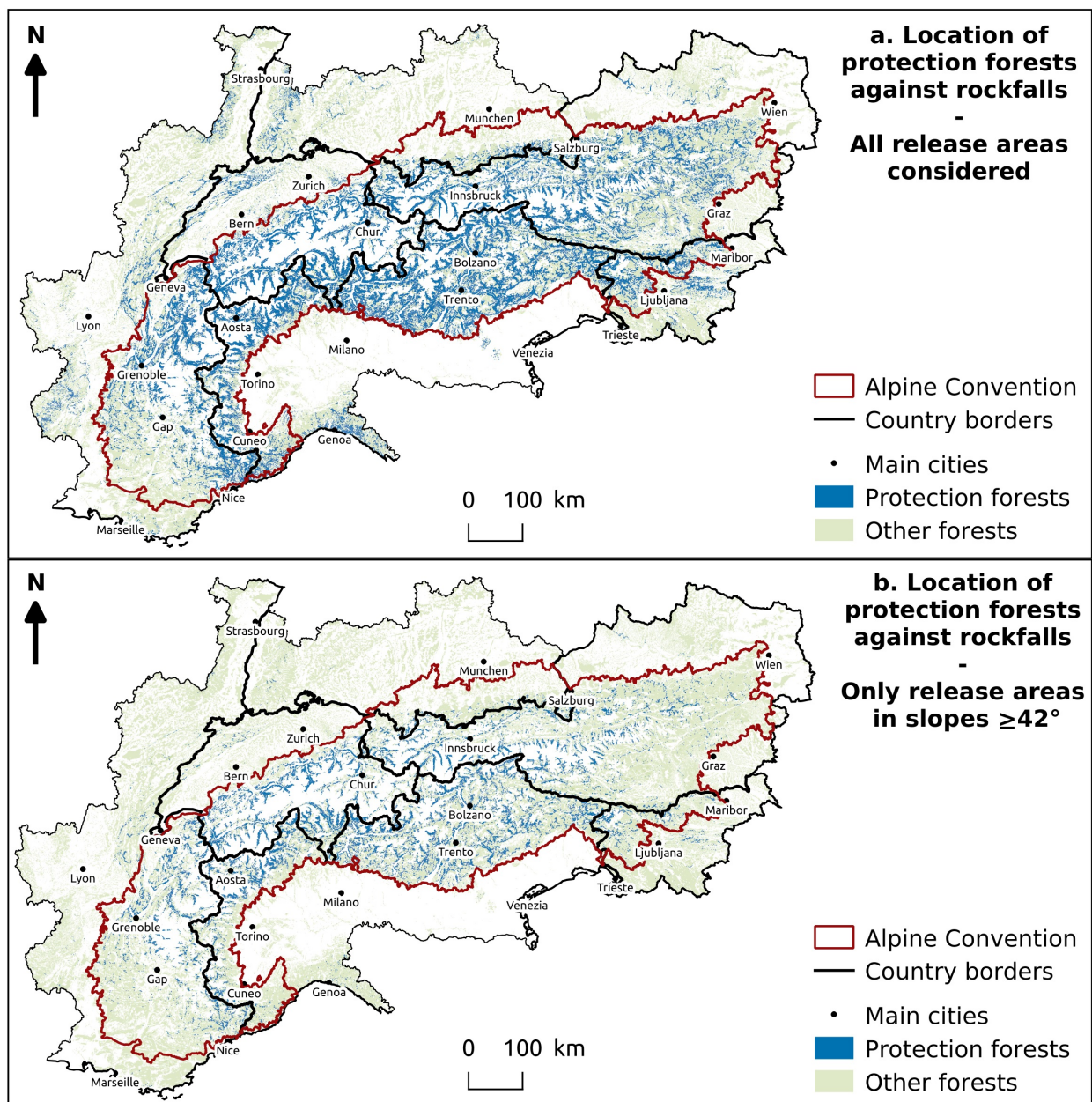


Figure 6: Location of the protection forests against rockfalls in the European Alps. Difference is made between protection forests identified with rockfall simulations from release areas located on slopes $\geq 42^\circ$ and those on slope in the range $[28-42^\circ]$.

3.2.1. Results at the country level

Generic results at the country level are provided in Table 5. The proportion of protection forest against rockfalls on the whole Alpine Space is in between 4.9% (while considering only potential release areas on slopes $\geq 42^\circ$) and 14% (all potential release areas included). The proportion is greater on the Alpine Convention region with a proportion in between 7.9% and 21.5% (according to the potential release areas considered).

The most mountainous countries (Switzerland, Italy and Liechtenstein) present the highest rate of protection forest against rockfall (>25% considering all release areas) while the flattest (Germany) presents only 3.3% of protection forest in the Alpine Space region. The proportion of protection forests are higher for all countries while considering only the Alpine Convention region (except Liechtenstein which is unchanged because completely included in the Alpine Convention), however, the hierarchy is unchanged with the mountainous countries presenting the highest rates.

Table 5: Results of the protection forest mapping at the country level for the entire Alpine Space region (a.) and the Alpine Convention region (b.). Difference is made between rockfall simulations from release areas located on slopes $\geq 42^\circ$ (suitable to the Alpine region) and those on slope in the range [28-42°].

a. Alpine Space region								
Country	Total area [km ²]	Release area density		Asset density [%]	Forest area [km ²]	Proportion of protection forest		
		28 – 42°	$\geq 42^\circ$			28 – 42°	$\geq 42^\circ$	Total
Austria	83 950	14.9%	2.5%	5.3%	37 280 (44.4%)	8.6%	3.7%	12.3%
Switzerland	41 290	19.3%	5.2%	9.8%	12 650 (30.6%)	13.6%	12.5%	26.1%
Germany	46 100	2.6%	0.4%	9.8%	16 410 (35.6%)	2.6%	0.7%	3.3%
France	101 440	8.6%	1.5%	10.2%	42 765 (42.2%)	6.0%	2.6%	8.6%
Italy	97 020	16.8%	3.6%	13.7%	35 165 (36.2%)	15.7%	9.0%	24.7%
Liechtenstein	160	25.0%	6.3%	13.9%	75 (46.9%)	16.0%	11.7%	27.8%
Slovenia	20 270	7.7%	1.2%	5.8%	11 810 (58.3%)	6.5%	1.9%	8.4%
Total	390 230	12.4%	2.5%	9.7%	156 155 (40.0%)	9.1%	4.9%	14.0%

b. Alpine Convention region								
Country	Total area [km ²]	Release area density		Asset density [%]	Forest area [km ²]	Proportion of protection forest		
		28 – 42°	$\geq 42^\circ$			28 – 42°	$\geq 42^\circ$	Total
Austria	54 630	22.9%	3.9%	3.7%	28 830 (52.8%)	10.9%	4.7%	15.6%
Switzerland	25 230	31.6%	8.5%	5.5%	7 610 (30.2%)	20.2%	20.4%	40.5%
Germany	11 150	10.9%	1.7%	3.0%	4 655 (41.7%)	4.8%	2.2%	7.1%
France	40 785	21.3%	3.7%	6.5%	19 365 (47.5%)	10.6%	5.4%	16.0%
Italy	52 030	31.3%	6.7%	11.9%	28 460 (54.7%)	18.2%	11.0%	29.2%
Liechtenstein	160	26.7%	6.5%	13.9%	75 (46.9%)	16.0%	11.7%	27.8%
Slovenia	6 770	23.2%	3.7%	3.4%	4 630 (68.4%)	11.7%	4.2%	15.9%
Total	190 755	25.3%	5.1%	6.8%	93 625 (49.1%)	13.5%	7.9%	21.5%

3.2.2. Results at the Alpine Space NUTS3 level

Detailed results at the NUTS3 level are provided in Fig. 7. The highest rates are observed in NUTS3 located in the Central Alps (maximum for the Uri Canton in Switzerland with 61% of protection forest considering all release areas). The proportion decreases slowly from the Central Alps to the Pre-Alps. No protection forest was identified for some NUTS3 located on flat areas such as the Po Valley in Italy or the plateau of South Germany.

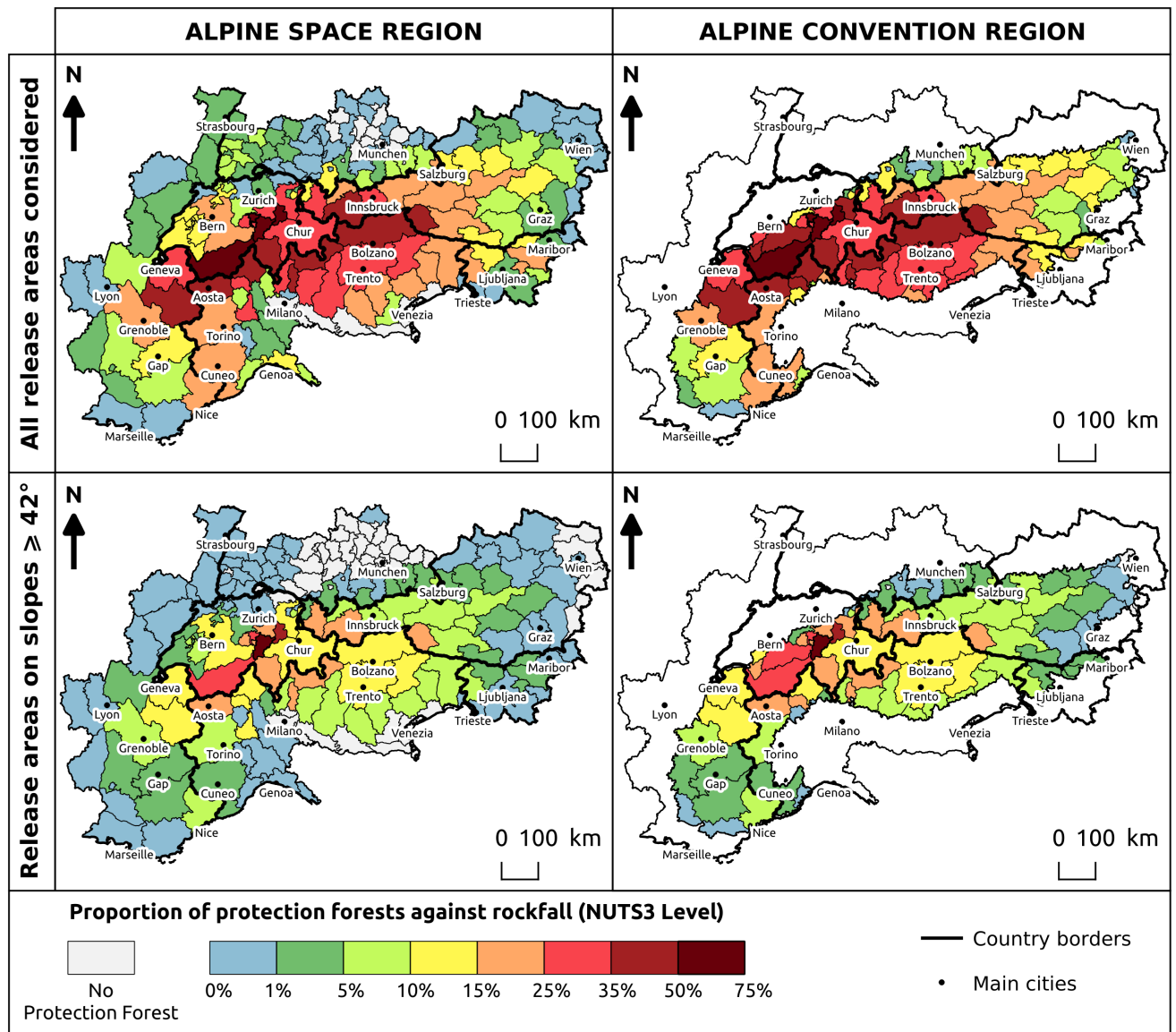


Figure 7: Maps of the proportion of protection forests against rockfalls according to the region considered (Alpine Space: left column – Alpine Convention: right column) and to the slope of the release area (all slopes considered: top row – Only release areas on slope $\geq 42^\circ$: bottom row). Proportions are calculated at the NUTS3 levels for both regions.

3.3. Which human assets are most often protected by forests?

In the Alpine region, road network is the human asset the most often encountered underneath protection forests. Thus, about 80% of the total area of the protection forests are located above roads (Table 6). Buildings are the second human asset type the most frequently protected by forests with about 55% of total area. Railways comes last with only 6% of the total protection forest area. If 63% of the protection forests concern a single human asset type, 34% of the them involve two different asset types and about 3% the three human asset types at the same time.

Table 6: Proportion of the human assets potentially affected by rockfall hazard for the entire Alpine Space region (a.) and the Alpine Convention region (b.). The proportion of protection forests that may mitigated rockfall hazard for each asset type is also returned. Difference is made between rockfall simulations from release areas located on slopes $\geq 42^\circ$ (suitable to the Alpine region) and those on slope in the range [28-42°].

a. Alpine Space region

Human asset type	Proportion of endangered asset			Proportion of the protection forests
	28 – 42°	42°	Total	
Railways	4.2%	2.3%	6.4%	5.8%
Buildings	2.4%	1.0%	3.4%	54.9%
Roads	4.3%	1.9%	6.2%	78.7%

b. Alpine Convention region

Human asset type	Proportion of endangered asset			Proportion of the protection forests
	28 – 42°	42°	Total	
Railways	10.6%	7.0%	17.6%	5.6%
Buildings	7.2%	3.3%	10.6%	56.4%
Roads	11.3%	5.8%	17.1%	78.2%

The total proportion of human assets potentially exposed to rockfall hazard in the Alpine Space region is relatively low with only 3.4% of buildings and 6% of railways and roads. However, when considering only the Alpine Convention region, the proportion is much higher with about 10% of the buildings and 17% of roads and highways.

4. Discussion

The method developed in this study allowed to build up the first harmonized map of protection forests against rockfalls for the whole European Alpine region. Established from open source data, the process is easily reproducible and could be replicated for others mountainous region as long as harmonized data of relief, land use and human assets are available. Based on harmonized inputs, the results authorize for the first time the comparison of the importance of protection forests against rockfall between the different countries of the Alpine region or smaller administrative entities such as NUTS3.

The presented approach has certain advantages over previous regional mappings of protection forests against rockfalls. For example, Switzerland is the only country to have a nationwide map of protection forests (Losey and Wehrli, 2013; Zinggeler, 1990) in the Alpine region. However, this map lies on a single rockfall simulation per source area. Our method uses a large number of rockfall simulations per source area (i.e. 500) in order to reflect the inherent randomness of any rockfall event (Bourrier et al., 2009) and to produce a more realistic covering of plausible rockfall trajectories. Another mapping method has been proposed by Toe and Berger (2015) and consists in extracting all straight terrain profiles from a digital terrain model from release area to the surrounding pixels that respect a threshold of energy line angle. Even if this allows fast calculation times, it does not account for topography and land use type in rock propagation and can lead to a wrong estimation of rockfall run out zones. In contrast, both topography and land use are essential to the process introduced in this paper. Land use participates to the calibration of soil parameters for the rockfall propagation, both topography and land use intervene in the validation of the simulations according to real rockfall events which ensures a robust modeling of potential rockfall trajectories.

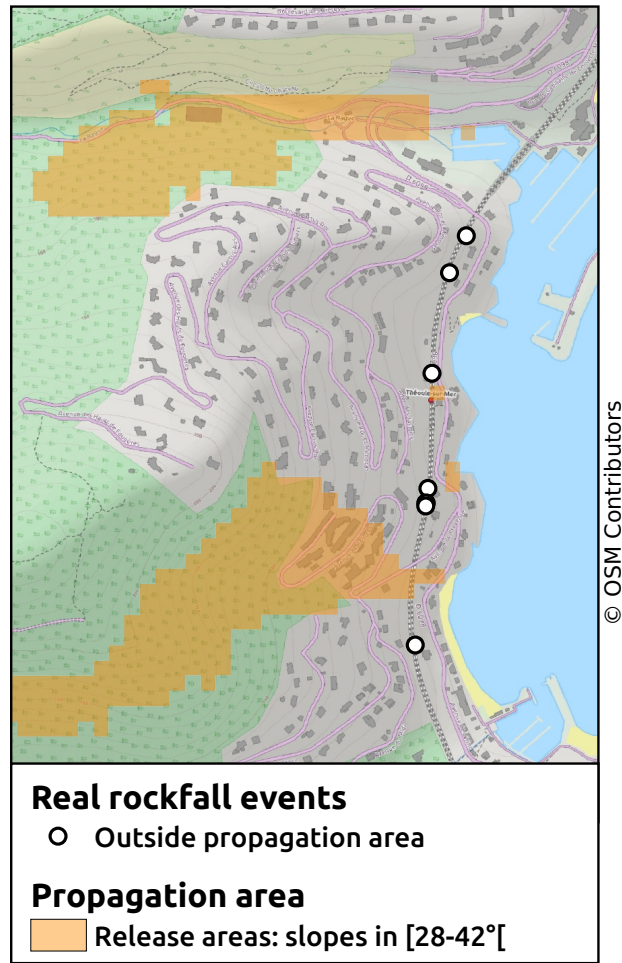


Figure 8: Examples of situation where real rockfall events are outside modeled propagation areas due to a non-detection of release areas in the South of France.

The accurate detection of rockfall release areas is one of the biggest challenges of a rockfall analysis on large areas (Michoud et al., 2012). The approach presented here integrates several slope thresholds for the detection of release areas. Rockfalls from release areas on slopes greater than or equal to the first threshold of 42° are more susceptible to occur (Fig. 5: about 65% of the real rockfalls events) especially in the most mountainous regions. The second threshold of 28° is mostly interesting in order to detect the release areas corresponding to small rocky barriers on short slopes which are poorly represented with a raster resolution of 25 m. This type of configuration is mainly found in the pre-Alps or in the middle mountains. Despite this, some release areas might not be detected as illustrated in Fig. 8 which explains that less than 5% of the real rockfall events present in the database were at a distance of the modeled rockfall propagation areas greater than 25 m. At the opposite, a part of the release areas identified in this work might not be active due to stable bedrock. To overcome this issue, it is possible to use a self-produced spatial layer of release areas instead of the default layer produced during the process.

The overall calculation time required to produce this map at the Alpine Space scale is about 256 days without multi-threading (43 days when considering only release areas on slopes greater than or equal to 42°). This figure must be qualified by the fact that 46.5 billion single simulations of rockfall propagation were computed which finally returns only 475 μ s per simulation. In order to overcome this issue, the computations were split on several threads on a server which allows us to get the results within two weeks of calculation. Moreover, it has to be said that the map does not need to be often updated, the same frequency as Corinne Land Cover updates should be sufficient (i.e every 6 years) in most of the Alpine region. However, in areas with very dynamic development, the appearance of new human

assets might imply that some forests become protection forests.

This work emphasizes that a significant proportion of mountain forests protect against rockfalls (up to 21.5% in the Alpine Convention region). However, managing these forests represents a cost that forest owners should not bear alone in view of the service it represents for mountain societies (Bianchi et al., 2018). By providing an objective and high resolution map of the forests having a potential to mitigate rockfall hazard at a large scale, this work could serve as a basis to implement a system of subsidies at the European scale to efficiently manage those forests and ensure that their protection capability will last or even improve in time. Such a system should rely on an objective evaluation of the protection capability of each forest identified here by using quantitative indicators (Dupire et al., 2016a,b). Remote sensing methods such as Lidar could also be of great interest in this topic (Monnet et al., 2017) in order to map the protective effect of each forest identified and be able to ensure a sustainable service of protection in the most efficient forest ecosystems.

Finally, the results of this study could be used as a means of communication and mediation with foresters, risk managers, local stakeholders in order to raise awareness about this important ecosystem service in mountain areas and to find innovative and consensual ways to sustainably manage these forests in a changing world.

5. Conclusion

This paper proposes an original method based on opensource data to map forests with a potential protection function against rockfalls for the entire European Alpine region. The reproducible approach developed in this work lies on an objective and robust calibration and validation process as well as a high number of 3-D simulations of rockfall trajectories over the Alps. The results of the harmonized mapping allow a precise identification of the forests endorsing a protection function against rockfall and reflect the important role that mountain forests play in protecting people and human assets from natural hazards.

Funding

This work was supported by the project RockTheAlps [grant n° ASP462] from the European Union's Interreg Alpine Space Programme.

References

- Accastello, C., Blanc, S., Brun, F., 2019. A framework for the integration of nature-based solutions into environmental risk management strategies. *Sustainability* 11 (2).
- Acosta, E., Agliardi, F., Crosta, G., Rios Aragues, S., 2007. Regional rockfall hazard assessment in the benasque valley (central pyrenees) using a 3d numerical approach. In: 4th EGS Plinius Conference–Mediterranean Storms. pp. 555–563.
- Bebi, P., Kienast, F., Schönenberger, W., 2001. Assessing structures in mountain forests as a basis for investigating the forests' dynamics and protective function. *Forest Ecology and Management* 145 (1-2), 3–14.
- Berger, F., Dorren, L. K., 2007. Principles of the tool Rockfor.net for quantifying the rockfall hazard below a protection forest. *Schweizerische Zeitschrift für Forstwesen* 158 (6), 157–165.
- Berger, F., Quetel, C., Dorren, L. K., 2002. Forest: a natural protection mean against rockfalls, but with which efficiency. In: *International Congress Interpraevent*. pp. 815–826.
- Bhattacharyya, A., 1946. On a measure of divergence between two multinomial populations. *Sankhyā: The Indian Journal of Statistics (1933-1960)* 7 (4), 401–406.
- Bianchi, E., Accastello, C., Trappmann, D., Blanc, S., Brun, F., 2018. The economic evaluation of forest protection service against rockfall: A review of experiences and approaches. *Ecological Economics* 154, 409 – 418.
- Bourrier, F., Berger, F., Tardif, P., Dorren, L., Hungr, O., 2012. Rockfall rebound: comparison of detailed field experiments and alternative modelling approaches. *Earth Surface Processes and Landforms* 37 (6), 656–665.
- Bourrier, F., Dorren, L., Nicot, F., Berger, F., Darve, F., 2009. Toward objective rockfall trajectory simulation using a stochastic impact model. *Geomorphology* 110 (3–4), 68–79.
- Brang, P., Schönenberger, W., Ott, E., Gardner, B., 2001. Forests as Protection from Natural Hazards. In: Evans, J. (Ed.), *The Forests Handbook*. Vol. 2. Blackwell Science Ltd., Oxford, pp. 53–81.
- Briner, S., Huber, R., Bebi, P., Elkin, C., Schmatz, D. R., Grêt-Regamey, A., 2013. Trade-Offs between Ecosystem Services in a Mountain Region. *Ecology and Society* 18 (3).
- Büttner, G., Kosztra, B., 2017. CORINE land cover 2018 technical guidelines. Tech. rep., European Environment Agency. Wien, Austria.
- Conedera, M., Krebs, P., Valsecchi, E., Cocca, G., Schunk, C., Menzel, A., Vacik, H., Cane, D., Japelj, A., Muri, B., Ricotta, C., Oliveri, S., Pezzatti, G., 2018. Characterizing alpine pyrogeography from fire statistics. *Applied Geography* 98, 87 – 99.

- Csilléry, K., Kunstler, G., Courbaud, B., Allard, D., Lassègues, P., Haslinger, K., Gardiner, B., 2017. Coupled effects of wind-storms and drought on tree mortality across 115 forest stands from the western alps and the jura mountains. *Global Change Biology* 23 (12), 5092–5107.
- Dorren, L. K., 2015. Rockyfor3D (v5.2) revealed - Transparent description of the complete 3D rockfall model. ecorisQ.
URL www.ecorisq.org
- Dorren, L. K., Maier, B., Putters, U. S., Seijmonsbergen, A. C., 2004. Combining field and modelling techniques to assess rockfall dynamics on a protection forest hillslope in the european alps. *Geomorphology* 57 (3), 151 – 167.
- Dorren, L. K., Seijmonsbergen, A. C., 2003. Comparison of three gis-based models for predicting rockfall runout zones at a regional scale. *Geomorphology* 56 (1), 49 – 64.
- Dorren, L. K. A., Berger, F., Putters, U. S., 2006. Real-size experiments and 3-D simulation of rockfall on forested and non-forested slopes. *Natural Hazards and Earth System Sciences* 6 (1), 145–153.
- Dumperth, C., Rohn, J., Fleer, A., Wang, J.-G., Xiang, W., Zimmermann, K., 2016. An easy approach to assess the susceptibility of a landslide by utilizing simple raster overlay methods: A case study on huangtupo landslide (p.r. china). *Journal of Mountain Science* 13 (10), 1701–1710.
- Dupire, S., Bourrier, F., Monnet, J.-M., Bigot, S., Borgniet, L., Berger, F., Curt, T., August 2016a. Novel quantitative indicators to characterize the protective effect of mountain forests against rockfall. *Ecological Indicators* 67, 98–107.
- Dupire, S., Bourrier, F., Monnet, J.-M., Bigot, S., Borgniet, L., Berger, F., Curt, T., December 2016b. The protective effect of forests against rockfalls across the French Alps: Influence of forest diversity. *Forest Ecology and Management* 382, 269–279.
- Dupire, S., Curt, T., Bigot, S., 2017. Spatio-temporal trends in fire weather in the french alps. *Science of The Total Environment* 595 (Supplement C), 801 – 817.
- Dupire, S., Curt, T., Bigot, S., Fréjaville, T., 2019. Vulnerability of forest ecosystems to fire in the french alps. *European Journal of Forest Research* 138 (5), 813–830.
- Francou, B., Manté, C., 1990. Analysis of the segmentation in the profile of alpine talus slopes. *Permafrost and Periglacial Processes* 1 (1), 53–60.
- Frattini, P., Crosta, G., Carrara, A., Agliardi, F., 2008. Assessment of rockfall susceptibility by integrating statistical and physically-based approaches. *Geomorphology* 94 (3), 419 – 437, gIS technology and models for assessing landslide hazard and risk.
- Gehring, E., Conedera, M., Maringer, J., Giadrossich, F., Guastini, E., Schwarz, M., 2019. Shallow landslide disposition in burnt European beech (*Fagus sylvatica* L.) forests. *Sci. Rep.* 9 (8638), 1–11.
- Getzner, M., Gutheil-Knopp-Kirchwald, G., Kreimer, E., Kirchmeir, H., Huber, M., 2017. Gravitational natural hazards: Valuing the protective function of alpine forests. *Forest Policy and Economics* 80, 150 – 159.
- Gobron, N., Pinty, B., Mélin, F., Taberner, M., Verstraete, M. M., Belward, A., Lavergne, T., Widlowski, J.-L., 2005. The state of vegetation in Europe following the 2003 drought. *International Journal of Remote Sensing* 26 (9), 2013–2020.
- Heim, A., 1932. Bergsturz und menschenleben. No. 20. Fretz & Wasmuth.
- Hollander, M., Wolfe, D. A., Chicken, E., 2013. *Nonparametric statistical methods*. John Wiley & Sons.
- Lepuschitz, E., 2015. Geographic information systems in mountain risk and disaster management. *Applied Geography* 63, 212 – 219.
- Losey, S., Wehrli, A., 2013. Forêt protectrice en suisse. du projet SilvaProtect-CH à la forêt protectrice harmonisée. Tech. rep., Office fédéral de l'environnement, Berne.
- Loye, A., Jaboyedoff, M., Pedrazzini, A., 2009. Identification of potential rockfall source areas at a regional scale using a dem-based geomorphometric analysis. *Natural Hazards and Earth System Sciences* 9 (5), 1643–1653.
- Meloni, M., Lingua, E., Motta, M., 2006. Analisi della funzione protettiva delle foreste: l'esempio della "Carta delle foreste di protezione diretta della Valle d'Aosta". *Forest@ - Journal of Silviculture and Forest Ecology* 3 (3), 420.
- Michoud, C., Derron, M.-H., Horton, P., Jaboyedoff, M., Baillifard, F.-J., Loye, A., Nicolet, P., Pedrazzini, A., Queyrel, A., 2012. Rockfall hazard and risk assessments along roads at a regional scale: example in swiss alps. *Natural Hazards and Earth System Sciences* 12 (3), 615–629.
- Monnet, J.-M., Bourrier, F., Dupire, S., Berger, F., 2017. Suitability of airborne laser scanning for the assessment of forest protection effect against rockfall. *Landslides* 14 (1), 299–310.
- Notaro, S., Paletto, A., 2012. The economic valuation of natural hazards in mountain forests: an approach based on the replacement cost method. *Journal of Forest Economics* 18 (4), 318–328.
- Pfeiffer, T. J., Bowen, T. D., 1989. Computer Simulation of Rockfalls. *Environmental and Engineering Geoscience* xxvi (1), 135–146.
- Toe, D., Berger, F., 2015. Regional Mapping of Forest with a Protection Function Against Rockfall. In: Lollino, G., Giordan, D., Crosta, G. B., Corominas, J., Azzam, R., Wasowski, J., Sciarra, N. (Eds.), *Engineering Geology for Society and Territory*. Vol. 2. Springer International Publishing, Cham, pp. 1957–1959.
- Volkwein, A., Schellenberg, K., Labiouse, V., Agliardi, F., Berger, F., Bourrier, F., Dorren, L., Gerber, W., Jaboyedoff, M., 2011. Rockfall characterisation and structural protection - a review. *Natural Hazards and Earth System Sciences* 11, p. 2617 – p. 2651.
- Wilcoxon, F., 1945. Individual comparisons by ranking methods. *Biometrics bulletin* 1 (6), 80–83.
- Zinggeler, A., 1990. Steinschlagsimulation in Gebirgswaldern. Modellierung der relevanten Teil-prozesse. Tech. rep., Geographisches Institut der Universität Bern. Switzerland.